

FINITE ELEMENT SIMULATION OF DRAPING WITH NON-CRIMP FABRICS

R.H.W. ten Thije and R. Akkerman

*University of Twente, Department of Mechanical Engineering, Composites Group
PO Box 217, 7500 AE, Enschede, the Netherlands.
Tel: +31 (0) 53 489 2426, email: r.h.w.tenthije@utwente.nl*

SUMMARY: The draping process of non-crimp fabrics (NCF) on a doubly curved mould determines the fibre distribution and hence the processing and performance of the NCF product. A composite Finite Element (FE) model is developed to simulate the draping process of NCFs on arbitrary geometries. Tool-part interaction is taken into account. Problem regions with possible fibre buckling can be indicated and the fibre distribution in the final NCF is predicted. The model contains a novel modelling approach to simulate the slip of the individual fibre layers. Additional layers and degrees of freedom were added to a membrane element to simulate the slipping layers with one element through the thickness. This enables efficient FE simulations of the draping process. Several experiments were performed: measurement of the thickness change during shear deformation, fibre pull-out experiments and a drape experiment. The latter is compared with FE simulations.

KEYWORDS: NCF, non-crimp fabric, draping, finite element, pull-out

INTRODUCTION

Resin infused composite products based on non-crimp fabrics (NCF) can offer a cost effective alternative for prepreg technology. These stitch-bonded fabrics can be draped like woven fabrics, but do not show a significant drop in mechanical performance due to the absence of fibre undulation. This makes them applicable for use in aerospace and automotive parts that demand a high mechanical performance. However, processability and performance are conflicting aspects in the development of the non-crimp fabric based composites. Easily drapeable and easily infusible NCFs often result in poor mechanical performance and vice versa. An optimal design can be achieved by modelling both processing and performance.

The process of draping the NCF on the mould plays a key role for components that exhibit double curvature. The fibre distribution after draping dominates both the filling process and the mechanical performance of the finished part. A Finite Element (FE) model is developed to simulate the draping process of NCFs on arbitrary geometries. The model identifies problem areas during the draping and it determines the fibre distribution in the final product. This allows for a numerical optimisation, reducing the production of costly prototypes.

NON-CRIMP FABRIC MATERIAL MODEL

This research focuses on non-crimp fabrics with a chain knit pattern. The resulting model can be adapted for non-crimp fabrics with different knit patterns by adjusting the stitch and shear behaviour. Five main deformation mechanisms can be identified in the chain knitted non-crimp fabric:

1. Extension and compaction of the stitch material
2. In-plane compaction of the yarns
3. Rotation of the yarns
4. Longitudinal extension and compaction of the fibres
5. Slip of the yarns

These deformation mechanisms are described in a continuum formulation, based on semi-empirical laws. The continuum formulation of the mechanisms 1 to 3 and corresponding experiments to obtain the material properties were reported in [1]. The longitudinal response of the fibres is linearly elastic according to Hook's law. The next section describes the slip mechanism of the yarns.

Slip of the yarns

The possibility of the individual yarns to slide through the stitches is an unconventional part of the deformation, when comparing to the more common woven fabrics. Woven fabrics can show a small amount of slip, but the effect is neglected in most drape simulations. Fibre slip is not negligible for non-crimp fabrics. Draping a non-crimp fabric on a doubly curved shape immediately shows the large influence of the mobility of the yarns.

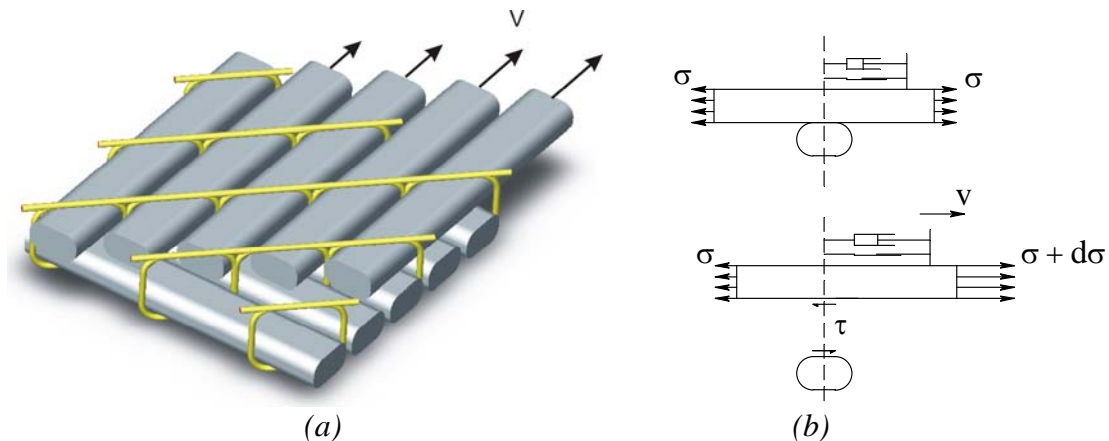


Fig. 1: (a) Slip of the yarns relative to the stitches and (b) the model with a Coulomb type and a viscous type of friction.

Fig. 1 illustrates the slip of the yarns in the top layer of a biaxial non-crimp fabric. A yarn is slipping through the stitches in its own longitudinal direction. Movement in the other two dimensions is restricted by either the other yarns or the stitches. The friction is partly of a Coulomb type and partly viscous. The total friction is assumed to be the sum of these two parts. Experiments illustrated that the friction is mainly of a Coulomb type, but a viscous part might be necessary for numerical stability during the FE simulation. The stress due to the friction acts in the direction of the slipping fibre. The slip velocity is the relative velocity of the fibres with respect to the stitches.

FINITE ELEMENT IMPLEMENTATION

The separate deformation mechanisms can be incorporated in a finite element formulation by using appropriate (nonlinear) constitutive laws. Continuum elements with nodal displacements as Degrees Of Freedom (DOF) are a common way to implement these constitutive laws. The slip mechanism obstructs a straightforward implementation of the complete material model by the use of constitutive laws and standard elements only. The material consists of different layers, all with individual displacements with respect to each other. Using multi-layer elements solves this problem.

Multi-layer element

The multi-layer element is based on a standard membrane element with a single continuum. Additional layers and additional degrees of freedom are added for each fibre layer. Fig. 2 shows an example of the element.

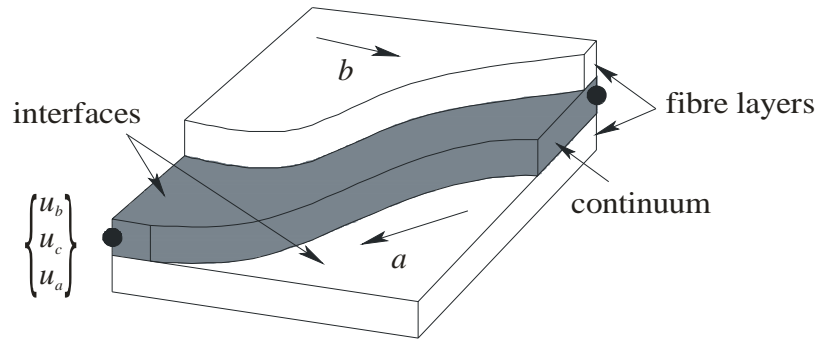


Fig. 2: A continuum element with two fibre layers. a and b are the fibre directions in the layers.

The underlying continuum layer has displacements as nodal degrees of freedom and incorporates the first three deformation mechanisms: the stitch response, the in-plane compaction response and the relative fibre rotation. The nodal displacements of this layer are equal to the stitch displacements. An additional layer is added to the element for each layer of fibres. This additional layer incorporates the longitudinal fibre deformation. The nodal degree of freedom for these layers is the displacement of the fibres in the fibre direction, relative to the stitches. The interface between the layers and the continuum experiences traction due to the slip of the fibres.

Element formulation

The element matrices for an element with two fibre layers are elaborated in this section. This element has a continuum layer and 2 fibre layers, as explained in the previous section. Without any additional layers, the element is equal to the normal membrane element with displacements in the x -, y - and z -direction as nodal degrees of freedom. Each fibre layer adds a nodal degree of freedom: the displacement of the fibre layer. This is a scalar value, because the fibre displacement is one-dimensional. The fibres can only slip in their own longitudinal direction. The total number of DOFs per node is 5 for the element with two fibre layers. The element is shown in Fig. 3. It is a one-dimensional version of the 3D element for simplicity. The element has 2 nodes: N^1 and N^2 .

The degrees of freedom are discretised in the standard way by using shape functions. The velocities are assumed constant during one increment. The relative displacements and velocities on the interfaces introduce a Coulomb type and a viscous type of traction. The

Coulomb type of traction is implemented with a small elastic part to increase the numerical stability. The local traction on a point on the interface is found by addition of the Coulomb part and the viscous part.

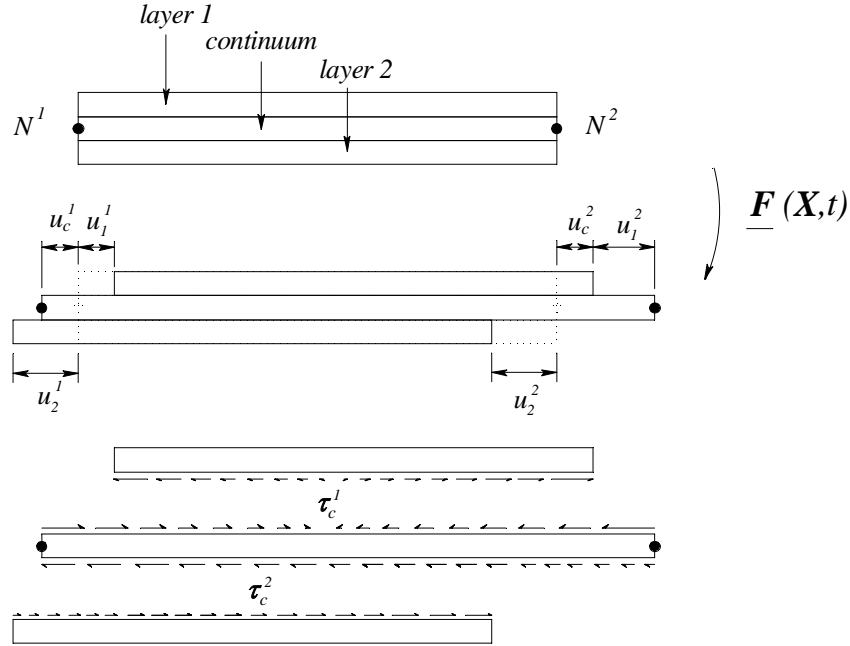


Fig. 3: Initial and deformed configuration of an element with 2 fibre layers.

The layers have zero relative displacement with respect to each other in the initial configuration. The element is deformed during the step and the layers slip due to this deformation. Slip introduces a frictional stress τ on the interfaces between the layers. Each layer has to fulfil the mechanical equilibrium. This results in three equations for this element. For the continuum layer, the weight equilibrium equation results in:

$$\int_{V_c} [N_c] \bar{\nabla} \sigma_c dV_c = -\sum_i \int_{S_i} [N_c] \tau_c^i dS_i \quad i = 1, 2 \quad (1)$$

where the matrix $[N]$ contains the element interpolation functions, σ_c denotes the internal stress in the continuum, V_c the volume of the continuum, τ_c^i the traction on the interface and S_i the interface surface. The index i denotes the fibre layer number. Each fibre layer i has to fulfil equilibrium as well:

$$\int_{V_i} [N_i] \bar{\nabla} \sigma_i dV_i = \int_{S_i} [N_i] \tau_c^i dS_i \quad i = 1, 2 \quad (2)$$

where σ_i denotes the internal stress in the layer and V_i the volume of the layer.

The subscript of the element interpolation functions denotes the coordinates on which the functions are based. The coordinates of the separate layers change during the step and this results in different interpolation functions for the different layers. Eqn.1 and Eqn. 2 must be satisfied at the end of each step. The implementation is done using an updated Lagrange procedure and solved using a Newton Rhapson scheme

There are limitations to this method. Material of the neighbouring elements slips into the element under consideration or vice versa and this is not taken into account. This effect is

considered negligible if the relative displacement of the layers during one step is small compared to the element size. If equilibrium is reached at the end of the step, the fibre layers are remapped to coincide with the continuum layer again. The simulation is then continued with the next increment. The advantage of this method is the absence of a contact search algorithm that locates the exact position of the fibre layers with respect to the continuum layer. This decreases the simulation time significantly.

MATERIAL CHARACTERISATION

A large number of experiments were performed to obtain the material parameters of the non-crimp fabric material model. This section describes two interesting experiments: trellis frame experiments with a constant thickness measurement and fibre pull-out experiments. All experiments were performed with a chain knitted biaxial ($\pm 45^\circ$) carbon non-crimp fabric with a polyester stitching thread, produced by Devold AMT. The used raw material is Tenax HTS 5631 12K carbon fibre. The thickness measurements in the trellis frame were done with type DB 540-C05+OB with an areal weight of 541 g/m^2 . The pull-out experiments were performed with type 2A DB with an areal weight of 538 g/m^2 . Both materials are almost identical, except for a minor difference in stitch distance and stitch tension.

Constant volume approach

The assumption of a constant volume during shear deformation is often used in numerical calculations on fabrics. To see whether this assumption is valid for the NCF fabric, trellis frame experiments with a continuous thickness measurement were performed to obtain accurate experimental data. The device used for measuring the thickness of the fabric during the experiment is found in figure 4a. It uses a Linear Variable Differential Transformer (LVDT) to measure displacements.

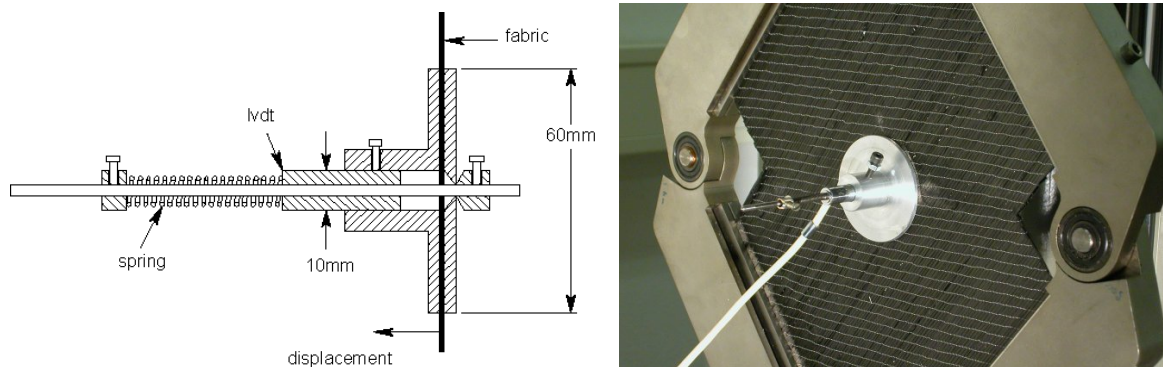


Fig. 4: (a) Device with an LVDT to measure the thickness of the fabric.
(b) The device mounted in the fabric.

The device consists of two circular plates that can slide along a rod. The right plate is blocked at the right side by a conical part. This allows tilting of a few degrees to assure that the right plate is parallel to the left plate. The fabric is locally distorted due to the rod penetrating the fabric. Therefore the inner 10 mm at the centre of the plates is removed. A small spring pushes the plates together. The spring was adjusted to a length where it delivers a pressure of 500 Pa on the fabric. The device can measure the thickness with an accuracy of $\pm 0.02 \text{ mm}$.

Fig. 5a shows the averaged results of the fabric thickness during an increasing shear angle. A total of three experiments were performed. The fabric was sheared up to approximately 63° during the experiment. This is the maximum shear angle the trellis frame could achieve due to

the size of the measuring device. The fit is based on the assumption of a constant volume ($T_0 = 0.84 \text{ mm}$). The fit starts at a shear angle of 0° . The initial fabric already has a shear angle of 8° . This suggests that the handling of the fabric before the start of the experiment already caused an initial shear angle. It is unknown whether this deformation is introduced during rolling after manufacturing or during unrolling before the experiment.

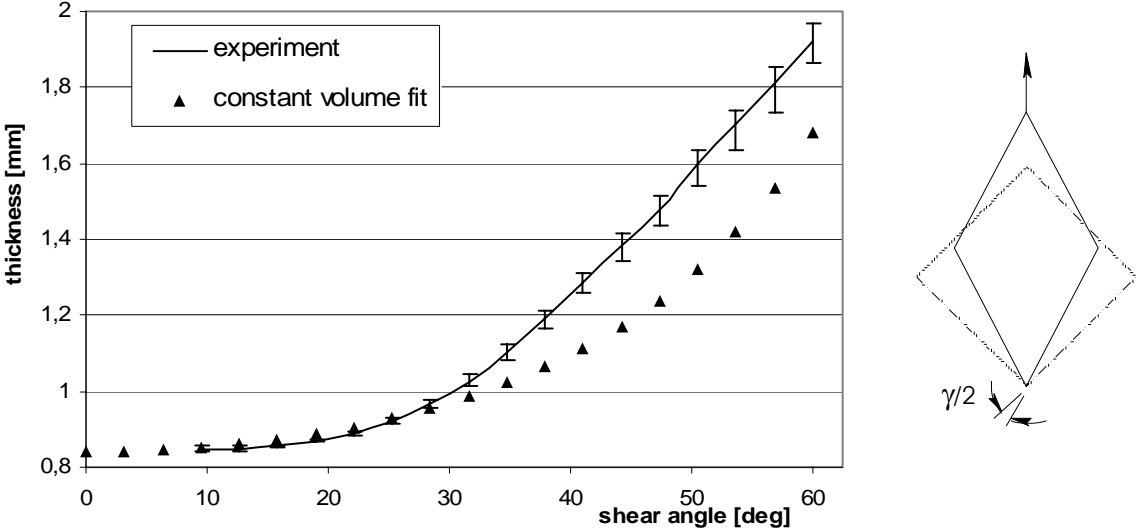


Fig. 5: (a) Averaged thickness of the fabric versus the shear angle for the first cycle and a fit assuming a constant volume. The error bars indicate the maximum and minimum value. (b) Definition of the shear angle.

Fig. 5a indicates that a constant volume assumption does not match the real deformation very well. A good match is only possible at low shear angles and shows a large deviation at high shear angles or vice versa. The experimental results indicate a dilatation effect. The thickness increases faster than expected based on a constant volume approach. The deviation at small shear angles is however small and in the assumption of a constant volume is used in the FE model during the simulations.

Fibre pull-out

Fibre pull-out experiments similar to those of Kong *et al.* [2] were performed to obtain the fibre slip parameters for the simulation. Fig. 6 shows the experimental setup and the dimensions of the sample.

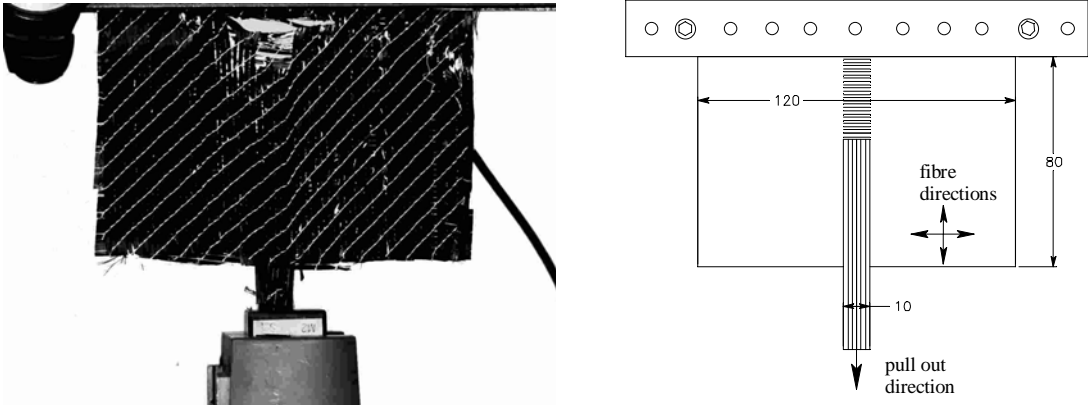


Fig. 6: Fibre pull-out experiment. Dimensions are in mm.

Kong et al. used a much smaller pull-out width, but here the larger width was chosen to minimise the influence of the edge effects observed at the interface between slipping and non-slipping fibres. It is impossible to restrict the pull-out of the fibres to the original pull-out width only. Fibres adjacent to the slipping fibres are partially pulled out and wrinkle. This increases the pull-out force. Experiments with smaller pull-out widths indicated that the edge effects are in an acceptable range of 5 to 10% for the 10 mm pull-out width.

The pull-out experiments were performed at three different velocities: 0.1, 1.0 and 10 mm/s. This was done to distinguish between the Coulomb type of friction and the viscous part. Three experiments were performed for each velocity. Fig. 7 shows the averaged results of the fibre pull-out experiments. The force is given per square mm of contact area between the fibre layers. It is assumed that the traction between the layers is equally distributed over this area. The results indicate that the friction between the layers is mainly of a Coulomb type below a pull-out length of 8 mm. The friction force steadily increases between 8 and 50 mm and a small velocity dependent part is observed. Above 50 mm the friction force levels.

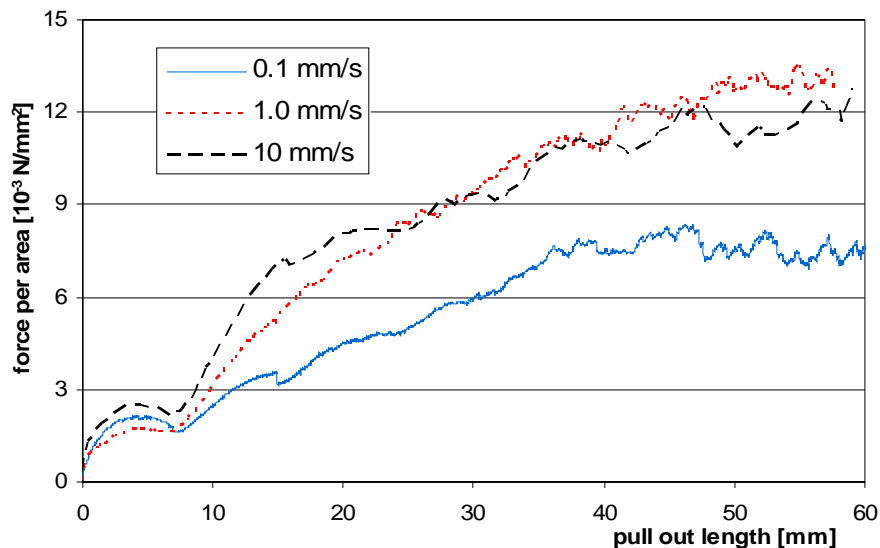


Fig. 7: Fibre pull-out results at different pull-out velocities.

The local minimum in the friction force at a pull-out length of 7 mm corresponds to the distance between 2 stitch rows. The perpendicular distance between two stitch rows is 5 mm. In the direction of the fibre, at 45° , this distance becomes approximately 7.1 mm ($5\sqrt{2}$). The end of the fibres slips through the stitch at this point and a small amount of elastic energy is released. The friction force increases after this local minimum. This has two causes. Firstly, the tension in the stitches increases during the pull-out experiment. This increases the contact force between the layers. Secondly, the undesired edge effects increase during the experiment.

Pull-out lengths during draping are normally smaller than 10 mm. The friction is assumed to be of a Coulomb type in this region. No significant velocity dependency is observed. The frictional force of the 1.0 mm/s experiment is even above the 0.1 mm/s experiment. This is attributed to the scatter in the experimental results. The Coulomb friction is implemented by using a yield stress of $2.0 \cdot 10^{-3}$ MPa: the average traction in the first part of the pull-out experiment as seen in Fig. 7. If the traction between the layers rises above this value, slip will occur. The friction is likely to be pressure dependent due to its Coulomb character, but this is not implemented in the FE model (yet).

DRAPE SIMULATION AND EXPERIMENT

Drape experiments and corresponding simulations were performed on a topped cone geometry. Fig. 8 shows the dimensions of the geometry, the setup of the simulation and the experimental setup.

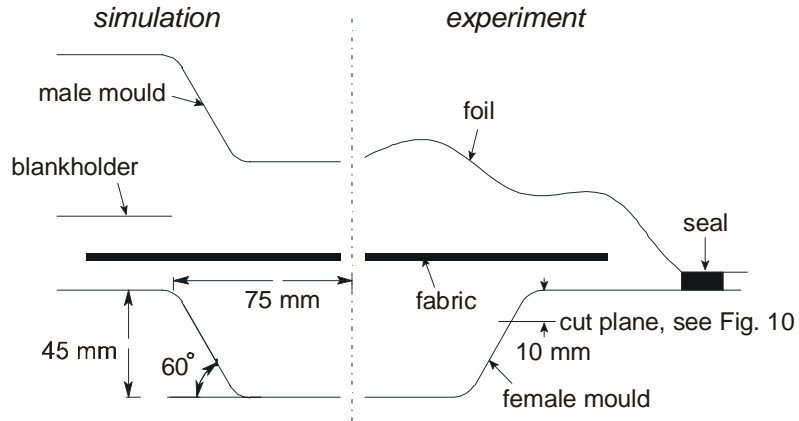


Fig. 8: Simulation setup and experimental setup (radii 10 mm).

The experimental product was manufactured with the Resin Injection under Flexible Tooling (RIFT) process. The simulation uses two moulds. This improves the numerical stability compared to shaping with only one mould and applying a pressure. The blankholder is modelled to simulate the effect of the vacuum that presses the fabric onto the mould. Simulations without a blankholder showed severe wrinkling in the fabric, which is also observed in experiments if the fabric is shaped with two hard moulds. Shaping under vacuum results in a more controllable way to perform the experiment.

The assumption of a constant volume is used, because the regions where shear angles exceed 30° to 35° are small. Although the experiments revealed that the friction between the fibre layers is mainly of a Coulomb type, the simulation was run with a viscous type of layer friction. The Coulomb type of friction was not fully implemented in the 3D FE simulation at that time.

A first simulation was done without tool-part friction and without a blankholder; a second one was done with a Coulomb type of friction between the part and the tool and a blankholder pressure. The values of the main simulation parameters can be found in Table 1. Fig. 9 shows the final part shape and the resulting fibre stresses at the end of the second simulation.

Table 1: Simulation parameters of the two different simulation.

		<i>Simulation 1</i>	<i>Simulation 2</i>
<i>Viscous friction coefficient between layers</i>	<i>Ns/mm³</i>	$1.45 \cdot 10^{-3}$	
<i>Mould closing speed</i>	<i>mm/s</i>	20.0	
<i>Blankholder pressure</i>	<i>bar</i>	<i>No</i>	0.15
<i>Tool-part friction coefficient</i>	-	<i>No</i>	0.20

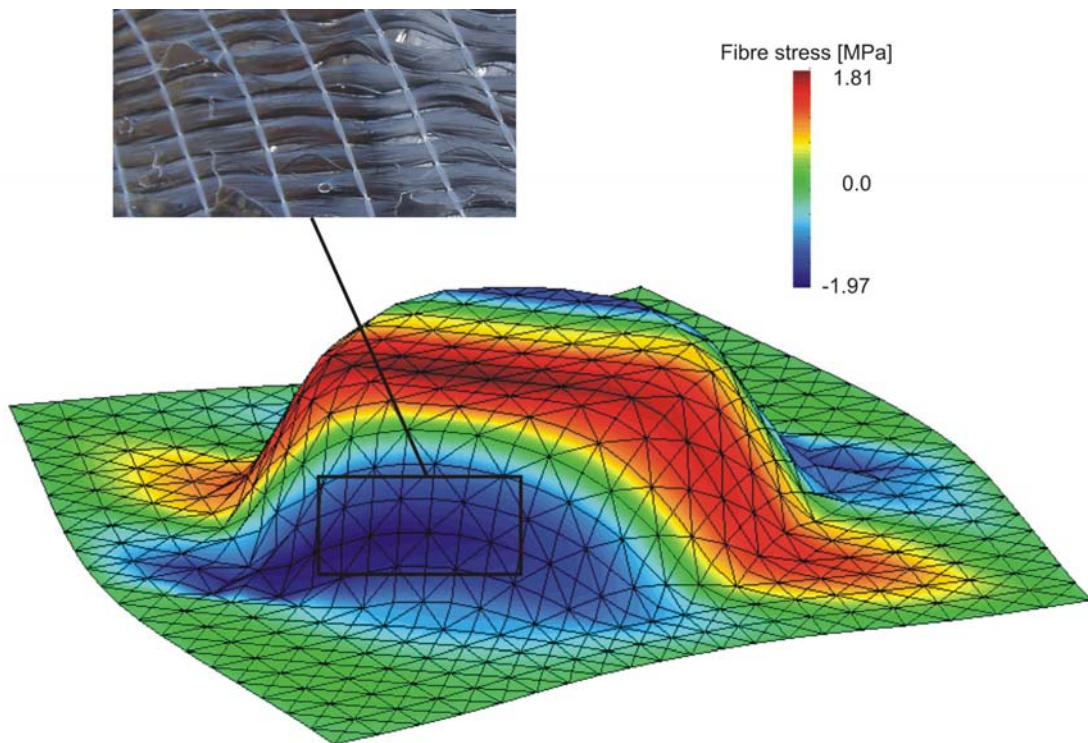


Fig. 9: Compressive fibre stresses predicted by the simulation and experimentally observed fibre buckling.

The regions with the highest compressive stresses correspond with the regions in the product where fibres start to buckle. Fig. 10 shows the enclosed fibre angle between the two fibre layers at a circular cross section on the cutting plane shown in Fig. 8. The results were obtained by taking pictures perpendicular to the surface at the inner and outer surface at an interval of 15° along the circular cross section. The pictures were analysed manually.

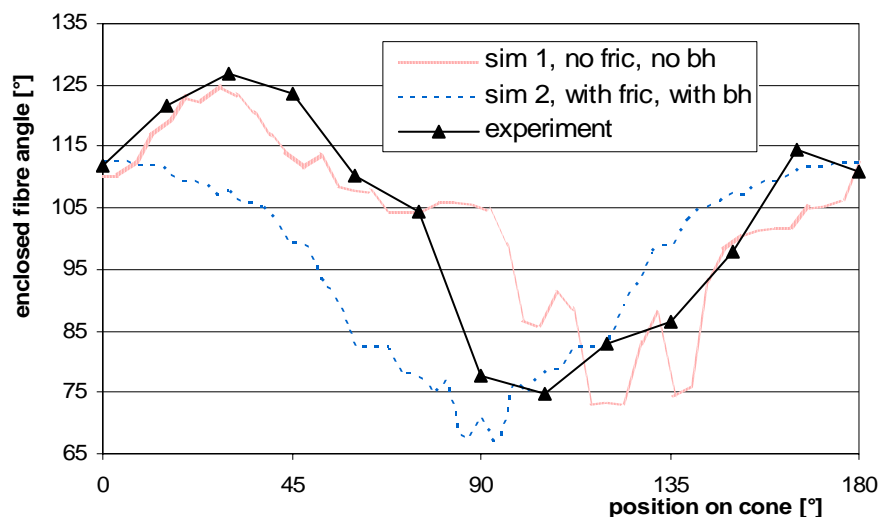


Fig. 10: Enclosed fibre angle in the cone drape experiment and two different FE simulations.

The results of simulation 2 are symmetrical due to the blankholder and the friction. The fabric remains in the middle of the mould. Simulation 1 and the experiment show non-symmetrical results mainly due to shifting and rotation of the fabric. The fabric is pulled into the mould from one side and not from all sides. This is very hard to control, which makes it difficult to compare simulations and experiments. The experimental procedure requires a re-designing of

the tooling to obtain more reproducible results. Nevertheless, the simulation results show a fairly good agreement for the zero friction case. The simulation captures the main trends observed in the experimental results.

CONCLUSIONS

A composite finite element model that simulates the draping of a non-crimp fabric on arbitrary geometries was developed and implemented. The model simulates the slip of the individual fibre layers with the use of one element through the thickness. Preliminary experimental results show that the model is capable of predicting the final fibre orientation with an accuracy of 10 to 15° and it identifies the regions that are susceptible to wrinkling due to compressive fibres stresses. More drape experiments and corresponding simulations need to be performed to validate the model.

Experimental work showed that the assumption of a constant fabric volume during shear is not correct for high shear angles. A significant dilatation effect is noticed at shear angles above 30 to 35°. Fibre pull-out experiments showed no significant velocity dependency.

A full 3D drape simulation was performed on a topped cone geometry. The simulation proves that a simulation of the draping process on an arbitrary geometry is possible. Verification of the results with corresponding reproducible drape experiments is the next step in the development of the FE model.

FUTURE WORK

The main part of the future works consists of validation of the model with drape experiments. The topped cone drape experiment discussed in this paper will be re-designed. The reproducibility is poor in the current configuration. A fabric with a grid printed on both sides will be used to improve the measurement of the enclosed fibre angles in the product. Drape experiments and simulations on more complex geometries, where problems like fibre bridging can occur, will be performed as well.

ACKNOWLEDGEMENTS

This work was performed with the support from the European Commission, by means of the FALCOM project (GRD1-2001-40184). This support is gratefully acknowledged by the authors

REFERENCES

1. R.H.W. ten Thije, R. Loendersloot and R. Akkerman, Material characterisation for finite element simulation of draping with non-crimp fabrics, *Proceedings on the 6th ESAFORM Conference on Material Forming*, Nuova Ipsa Editore, Palermo, 2003.
2. H. Kong, A.P. Mouritz and R. Paton, Tensile extension properties and deformation mechanisms of multiaxial non-crimp fabrics, *Composite Structures* 66 (2004), p249–259.